

Excitation of ${}^3P(2p)^2$ state of helium by electron impact

A. C. Roy* and N. C. Sil

Department of Theoretical Physics, Indian Association for the Cultivation of Science, Calcutta 700032, India

(Received 23 December 1975)

Close-coupling cross sections for the electron-impact parity-unfavored transition ${}^3P(2p)^2 \leftarrow {}^1S(1s)^2$ in helium are calculated in an integral equation approach. At an energy 0.11 eV above threshold the present formalism yields a cross section of $1.55 \times 10^{-4} a_0^2$ which is in good agreement with experiment. Our calculated slope at this energy is $6 \times 10^{-20} \text{ cm}^2/\text{eV}$ against an experimental value of $4 \times 10^{-20} \text{ cm}^2/\text{eV}$. The present cross sections satisfy the threshold law for parity-unfavored transitions. A Born-Oppenheimer (BO) calculation is also performed, and it is found that near threshold BO cross sections are too small in comparison with experimental results. The dependence of BO cross sections on the choice of atomic wave functions is also examined.

I. INTRODUCTION

The electron-impact ${}^3P(2p)^2 \leftarrow {}^1S(1s)^2$ transition in helium was first studied by Becker and Dahler.^{1,2} They examined this transition process in the Born-Oppenheimer (BO), distorted-wave (DW), and close-coupling (CC) methods and observed that of the three methods, the last two gave identical cross sections and that the BO cross sections were in substantial agreement with those obtained from the more sophisticated DW and CC methods. Recently, Burrow³ applied the trapped-electron method and measured cross sections for the above-mentioned transition near threshold. He remarked that at an energy 0.11 eV above threshold, the cross sections obtained from the calculations of Becker and Dahler² differed greatly from his measured values. Since Becker and Dahler² adopted for the doubly excited eigenstate an eigenenergy which differed considerably from the experimental value, their calculated cross sections are unlikely to be reliable near threshold. So with the availability of experimental results in the vicinity of threshold, there is clearly a need to look at this problem again from a critical angle.

The present paper reports the results of the application of the integral form of the close-coupling approximation⁴⁻⁸ to the electron-impact ${}^3P(2p)^2 \leftarrow {}^1S(1s)^2$ transition in helium. This integral form of the close-coupling approximation differs from the conventional form⁹ of CC in that instead of integrodifferential equations one solves here integral equations with the boundary conditions automatically incorporated. Since our main purpose is to evaluate reliable cross sections close to threshold, we have used in the present calculation accurate energy eigenvalues for the target eigenstates. Only two bound states, namely, the initial and final states of the target atom, are included. For the initial state Hartree-

Fock atomic orbitals are adopted, whereas for the final state we have chosen hydrogenic orbitals. The close-coupling equations are solved by an algebraic method.^{5,6} The resulting cross sections are compared with the corresponding theoretical and experimental values. Simple BO calculations^{10,11} are also performed using different atomic wave functions, and the dependence of cross sections on the choice of wave functions is examined. Furthermore, threshold behavior of cross sections for this parity-unfavored transition¹² is reported.

In Sec. II the integral form of the close-coupling method is formulated for the present case of double excitation of helium. The explicit expressions for the close-coupled equations are given. Section III contains an analysis of results. Concluding remarks are made in Sec. IV. The Appendix deals with the evaluation of partial-wave matrix elements which appear in the coupled equations. Atomic units are used throughout the paper.

II. THEORY

The integral method of the close-coupling approximation has been described in detail in a number of papers.⁴⁻⁸ In this section we present a brief formulation of the above method as applied to the ${}^3P(2p)^2 \leftarrow {}^1S(1s)^2$ transition in helium. In the present formalism only the initial and final states of the target wave function will be retained in the expansion of the total wave function of the system consisting of the scattering electron and the target. The antisymmetrized total wave function¹³ may then be written as

$$\Psi(1, 2, 3) = \sum_{\text{cyc}} [\phi_{1+}(1, 2)F_{1+}(3)\chi_{-}(1, 2; 3) + \phi_{2-}(1, 2)F_{2-}(3)\chi_{+}(1, 2; 3)]. \quad (1)$$

Here $F_{1+}(3)$ and $F_{2-}(3)$ denote the wave functions

for the scattered electron, which are associated with the initial and final states, respectively. ϕ_{1+} and ϕ_{2-} refer to the coordinate wave functions of target atom, and χ_+ and χ_- are the appropriate spin wave functions.^{14, 15} The signs + and - denote symmetry and antisymmetry, respectively. The symbol \sum_{cyc} stands for a permutation operator which ensures that $\Psi(1, 2, 3)$ is antisymmetric with respect to the interchange of any pair of electrons.

Following Drukarev¹⁶ we obtain in the present case a pair of coupled integrodifferential equations describing the scattering of electrons from atomic helium,

$$(E - E_{1+}^{(b)} - T_3)F_{1+}(3) = \hat{V}_{11}^{++}F_{1+}(3) + \hat{V}_{12}^{+-}F_{2-}(3), \quad (2)$$

$$(E - E_{2-}^{(b)} - T_3)F_{2-}(3) = \hat{V}_{22}^{--}F_{2-}(3) + \hat{V}_{21}^{-+}F_{1+}(3). \quad (3)$$

In a compact notation, Eqs. (2) and (3) can be expressed as

$$(E - E_{\alpha'}^{(b)} - T_3)F_{\alpha'}(3) = \sum_{\alpha=1}^2 \hat{V}_{\alpha'\alpha}^{\alpha'\alpha} F_{\alpha}(3). \quad (4)$$

Here E is the total energy of the system, T_3 the kinetic energy operator for electron 3, $E_{\alpha'}^{(b)}$ the energy of target atom in state α' , α' denotes the symmetry (+ or -) of the target eigenstate, and \hat{V} stands for an operator in a two-body Hilbert space. The operators \hat{V}_{11}^{++} , \hat{V}_{12}^{+-} , \hat{V}_{22}^{--} , and \hat{V}_{21}^{-+} are defined as follows:

$$\begin{aligned} \hat{V}_{11}^{++} = & \int d\vec{r}_1 d\vec{r}_2 \phi_{1+}^*(1, 2) \left(-\frac{2}{r_3} + \frac{2}{r_{31}} \right) \phi_{1+}(1, 2) \\ & - \int d\vec{r}_1 d\vec{r}_2 \phi_{1+}^*(1, 2) (H - E) \phi_{1+}(2, 3), \quad (5) \end{aligned}$$

$$\hat{V}_{12}^{+-} = 3^{1/2} \int d\vec{r}_1 d\vec{r}_2 \phi_{1+}^*(1, 2) (H - E) \phi_{2-}(3, 2), \quad (6)$$

$$\begin{aligned} \hat{V}_{22}^{--} = & \int d\vec{r}_1 d\vec{r}_2 \phi_{2-}^*(1, 2) \left(-\frac{2}{r_3} + \frac{2}{r_{31}} \right) \phi_{2-}(1, 2) \\ & - \int d\vec{r}_1 d\vec{r}_2 \phi_{2-}^*(1, 2) (H - E) \phi_{2-}(2, 3), \quad (7) \end{aligned}$$

$$\hat{V}_{21}^{-+} = 3^{1/2} \int d\vec{r}_1 d\vec{r}_2 \phi_{2-}^*(1, 2) (H - E) \phi_{1+}(2, 3). \quad (8)$$

The Hamiltonian H is given by

$$\begin{aligned} H = & T_1 + T_2 + T_3 \\ & - 2 \left(\frac{1}{r_1} + \frac{1}{r_2} + \frac{1}{r_3} \right) + \frac{1}{r_{12}} + \frac{1}{r_{23}} + \frac{1}{r_{31}} - E. \quad (9) \end{aligned}$$

Following Sloan and Moore,⁴ the close-coupling equations (4) can be converted into equivalent integral equations and the three-body transition

amplitude can be written

$$\begin{aligned} \langle \vec{k}' \alpha' | T | \vec{k} \alpha \rangle = & \langle \vec{k}' \alpha' | B | \vec{k} \alpha \rangle \\ & + \sum_{\alpha''} \int d\vec{k}'' \frac{\langle \vec{k}' \alpha' | B | \vec{k}'' \alpha'' \rangle \langle \vec{k}'' \alpha'' | T | \vec{k} \alpha \rangle}{E + i\epsilon - E_{\alpha''}}. \quad (10) \end{aligned}$$

Here T and B are the three- and two-body operators, respectively, and $\langle \vec{k}' \alpha' | T | \vec{k} \alpha \rangle$ denotes the amplitude for transition from state α to state α' , with \vec{k} and \vec{k}' the initial and final momenta. α is characterized by the principal quantum number n , the orbital-angular-momentum quantum number l_a and the projection quantum number m_a of the target atom. The summation over α'' stands for the two states, namely, the initial state 1 and the final state 2, which are retained in the expansion of total wave function of the system. $E_{\alpha''}$ is given by

$$E_{\alpha''} = \frac{1}{2} k''^2 + E_{\alpha''}^{(b)},$$

where $E_{\alpha''}^{(b)}$ is the energy of target atom in state α'' .

We express the two-body transition amplitude as

$$\langle \vec{k}' \alpha' | B | \vec{k} \alpha \rangle = - (1/4\pi^2) f_{\alpha'\alpha}^B(\hat{k}', \hat{k}), \quad (11)$$

where

$$\begin{aligned} f_{\alpha'\alpha}^B(\hat{k}', \hat{k}) = & \frac{3^{1/2}}{2\pi} \int d\vec{r}_1 d\vec{r}_2 d\vec{r}_3 \phi_{\alpha'}^*(\vec{r}_1, \vec{r}_2) e^{-i\vec{k}' \cdot \vec{r}_3} \\ & \times (H - E) \phi_{\alpha}(\vec{r}_2, \vec{r}_3) e^{i\vec{k} \cdot \vec{r}_1}. \quad (12) \end{aligned}$$

On the energy shell, $f_{\alpha'\alpha}^B(\hat{k}', \hat{k})$ becomes the BO scattering amplitude.¹

In the present calculations we have used two different forms (form A and form B) of approximate atomic wave functions. These are as follows:

Form A.

$$\begin{aligned} ^3P(2p)^2: \psi^{(m)}(12) \\ = \sum_{\nu} C(1, 1, 1; \nu, m - \nu, m) \psi_{21\nu}(\gamma, 1) \psi_{21, m-\nu}(\gamma, 2), \end{aligned}$$

$$\begin{aligned} ^1S(1s)^2: \psi_0(23) \\ = N[\psi_{100}(\alpha, 2) \psi_{100}(\beta, 3) + \psi_{100}(\alpha, 3) \psi_{100}(\beta, 2)]. \end{aligned}$$

Form B. $^3P(2p)^2: \psi^{(m)}(12)$ is the same as in form A;

$$^1S(1s)^2: \psi_0(23) = \phi_0(r_2) \phi_0(r_3),$$

where

$$\phi_0(r) = (4\pi)^{-1/2} (A e^{-\lambda r} + B e^{-\mu r}).$$

Form A consists of hydrogenic wave functions as adopted by Becker and Dahler,² while in form B the ground-state wave function of helium is

taken to be the Hartree-Fock function of Byron and Joachain.¹⁷

The three-body matrix element is expressed in the same way as (12):

$$\langle \bar{k}'\alpha' | T | \bar{k}\alpha \rangle = -(1/4\pi^2) f_{\alpha'\alpha}(\hat{k}', \hat{k}) \quad (13)$$

where $f_{\alpha'\alpha}(\hat{k}', \hat{k})$ represents the scattering amplitude.

Now we make the partial-wave expansion of the three-body transition amplitude,

$$\langle \bar{k}'n'l'_am'_a | T | \bar{k}nl_a \rangle = \frac{N'}{(kk')^{1/2}} \sum_{LM} \sum_{l'm'} \sum_{l''m''} \langle l'l'_am'_a | LM \rangle Y_{l'm'}(\hat{k}') T^L(k'n'l'_a; knll_a) \langle ll_a mm_a | LM \rangle Y_{lm}^*(\hat{k}), \quad (14)$$

with $N' = 1/2\pi$. Here $T^L(k'n'l'_a; knll_a)$ are the conveniently normalized partial-wave T -matrix elements, and the m are the orbital angular momentum and magnetic quantum numbers, respectively, of the free particle, L is the total angular momentum of the system consisting of the scattering electron and the target, and M is its z component. $Y_{lm}(\hat{k})$ and $\langle ll_a mm_a | LM \rangle$ denote, respectively, the spherical harmonic and the Clebsch-Gordan coefficient.

Let us denote, for convenience, the set of quantum numbers (nl_a) as τ . Now using an expansion similar to (14) for the two-body transition amplitude, substituting (14) into Eq. (10), and utilizing the orthogonal properties of spherical harmonics and of Clebsch-Gordan coefficients, the three-dimensional integral equations can be reduced to one-dimensional equations,

$$T^L(k'\tau'; k\tau) = B^L(k'\tau'; k\tau) + N' \sum_{\tau''} \int dk'' k'' (E + i\epsilon - E_{\tau''})^{-1} B^L(k'\tau'; k''\tau'') T^L(k''\tau''; k\tau). \quad (15)$$

We divide the pole term into a δ -function part and a principal-value part,

$$(E + i\epsilon - E_{\tau''})^{-1} = -i\pi\delta(E - E_{\tau''}) + P(E - E_{\tau''})^{-1}. \quad (16)$$

Equation (15) then becomes

$$\begin{aligned} T^L(k'\tau'; k\tau) &= B^L(k'\tau'; k\tau) - i\pi N' \sum_{\tau''} B^L(k'\tau'; k_{\tau''}\tau'') T^L(k_{\tau''}\tau''; k\tau) \\ &+ P N' \sum_{\tau''} \int dk'' k'' \frac{1}{\frac{1}{2}(k_{\tau''}^2 - k''^2)} B^L(k'\tau'; k''\tau'') T^L(k''\tau''; k\tau), \end{aligned} \quad (17)$$

with

$$k_{\tau''}^2 = k^2 + 2(E_1^{(0)} - E_{\tau''}^{(0)}). \quad (18)$$

$E_1^{(0)}$ and $E_{\tau''}^{(0)}$ are the energies of the target in the ground and τ'' states, respectively.

In the present case of double excitation, only one partial wave² ($l=l'=L=1$) contributes to the cross section. A detailed explanation is given in Appendix.

The close-coupled equations are then written

$$\begin{aligned} T^1(k', 2, 1, 1; k, 1, 1, 0) &= B^1(k', 2, 1, 1; k, 1, 1, 0) - i\pi N' [B^1(k', 2, 1, 1; k_1, 1, 1, 0) T^1(k_1, 1, 1, 0; k, 1, 1, 0) \\ &+ B^1(k', 2, 1, 1; k_2, 2, 1, 1) T^1(k_2, 2, 1, 1; k, 1, 1, 0)] \\ &+ P N' \int dk'' k'' \left(\frac{1}{\frac{1}{2}(k_1^2 - k''^2)} B^1(k', 2, 1, 1; k'', 1, 1, 0) T^1(k'', 1, 1, 0; k, 1, 1, 0) \right. \\ &\left. + \frac{1}{\frac{1}{2}(k_2^2 - k''^2)} B^1(k', 2, 1, 1; k'', 2, 1, 1) T^1(k'', 2, 1, 1; k, 1, 1, 0) \right), \end{aligned} \quad (19)$$

$$\begin{aligned} T^1(k', 1, 1, 0; k, 1, 1, 0) &= B^1(k', 1, 1, 0; k, 1, 1, 0) - i\pi N' [B^1(k', 1, 1, 0; k_1, 1, 1, 0) T^1(k_1, 1, 1, 0; k, 1, 1, 0) \\ &+ B^1(k', 1, 1, 0; k_2, 2, 1, 1) T^1(k_2, 2, 1, 1; k, 1, 1, 0)] \end{aligned}$$

$$\begin{aligned} &+ P N' \int dk'' k'' \left(\frac{1}{\frac{1}{2}(k_1^2 - k''^2)} B^1(k', 1, 1, 0; k'', 1, 1, 0) T^1(k'', 1, 1, 0; k, 1, 1, 0) \right. \\ &\left. + \frac{1}{\frac{1}{2}(k_2^2 - k''^2)} B^1(k', 1, 1, 0; k'', 2, 1, 1) T^1(k'', 2, 1, 1; k, 1, 1, 0) \right). \end{aligned} \quad (20)$$

The differential cross section $I(\theta, \phi)$ for the transition process ${}^3P(2p)^2 \leftarrow {}^1S(1s)^2$ can be obtained from the relation (13) by using the partial-wave expansion (14). A simple algebraic calculation gives

$$I(\theta, \phi) = (9/8k^2) |T^1(k', 2, 1, 1; k, 1, 1, 0)|^2 \sin^2 \theta. \quad (21)$$

The total cross section $\sigma(n', l'_a \leftarrow n, l_a)$ is given by

$$\sigma(2, 1 \leftarrow 1, 0) = (3\pi/k^2) |T^1(k', 2, 1, 1; k, 1, 1, 0)|^2. \quad (22)$$

III. ANALYSIS OF RESULTS

A. Born-Oppenheimer calculation

BO cross section (Table I) are evaluated from the formulas given by Becker and Dahler² using two different forms of approximate atomic wave

functions. In Fig. 1 are displayed these cross sections of present calculations, together with those of Becker and Dahler.² Curve A shows the cross sections of Becker and Dahler calculated using hydrogenic wave functions (form A) and theoretical eigenenergies. Curve B of the present calculations differs from curve A in that experimental eigenenergies are used here. Curve C gives the present cross sections computed from the Hartree-Fock and hydrogenic wave functions (form B) for the ground and excited states, respectively, of helium (experimental eigenenergies are used). Hereafter, calculations yielding curves A, B, and C will be referred to as calculations A, B, and C, respectively.

We have recalculated the BO cross sections of Becker and Dahler for ${}^3P_g(2p)^2 \leftarrow {}^1S_g(1s)^2$ transition in helium. Apparently, there is an error in the

TABLE I. Cross sections for the electron-impact ${}^3P(2p)^2 \leftarrow {}^1S(1s)^2$ transition in helium, in units of a_0^2 .

Energy (eV)	Present work				
	BO ^a	BO ^b	BO ^c	CC	Experiment ^d
59.65	0.1772(-4) ^e	0.6995(-7)	0.9271(-7)	0.352(-5)	...
59.67	0.1896(-4)	0.3535(-6)	0.4760(-6)
59.70	0.2083(-4)	0.9870(-6)	0.1335(-5)
59.72	0.2212(-4)	0.1523(-5)	0.2043(-5)
59.74	0.2342(-4)	0.2117(-5)	0.2843(-5)	0.134(-3)	...
59.75	0.2409(-4)	0.2432(-5)	0.3276(-5)	0.155(-3)	0.157(-3)
59.76	0.2474(-4)	0.2766(-5)	0.3734(-5)	0.178(-3)	...
59.78	0.2608(-4)	0.3478(-5)	0.4686(-5)
59.80	0.2744(-4)	0.4238(-5)	0.5705(-5)
59.85	0.8516(-5)	0.418(-3)	...
60.0	0.4188(-4)	0.1386(-4)	0.1866(-4)
60.5	...	0.4747(-4)	0.6375(-4)
61.0	...	0.8754(-4)	0.1173(-3)	0.127(-1)	...
61.6	0.1787(-3)	0.1385(-3)	0.1853(-3)
62.0	0.2130(-3)	0.1726(-3)	0.2305(-3)	0.657(-1)	...
62.6	0.2621(-3)	0.2222(-3)	0.2959(-3)
63.0	0.2929(-3)	0.2537(-3)	0.3372(-3)	0.561(-1)	...
63.5	0.3289(-3)	0.2908(-3)	0.3857(-3)
64.0	0.3619(-3)	0.3253(-3)	0.4304(-3)	0.162(-1)	...
65.0	0.4191(-3)	0.3856(-3)	0.5078(-3)
67.0	0.4996(-3)	0.4727(-3)	0.6162(-3)	0.134(-2)	...
70.0	0.5519(-3)	0.5336(-3)	0.6846(-3)
72.0	0.5547(-3)	0.5407(-3)	0.6865(-3)
75.0	0.5295(-3)	0.5205(-3)	0.6503(-3)	0.123(-3)	...
80.0	0.4507(-3)	0.4466(-3)	0.5438(-3)
90.0	0.2844(-3)	0.2828(-3)	0.3285(-3)
100.0	0.1666(-3)	0.1669(-3)	0.1863(-3)
120.0	0.5661(-4)	0.5686(-4)	0.5966(-4)
150.0	0.1246(-4)	0.1253(-4)	0.1240(-4)

^a Calculation A (see Sec. IIIA); BO cross sections of Ref. 2.

^b Calculation B (see Sec. IIIA); present BO cross sections using form-A wave functions.

^c Calculation C (see Sec. IIIA); present BO cross sections using form-B wave functions.

^d Experimental cross section of Ref. 3.

^e The number in parentheses denotes the power of 10 by which the preceding number is to be multiplied.

expression for $f_1(\theta, \phi; {}^3P_g)$ in Ref. 2 [Eq. (4), p. A75] due to transcription, because the reported results are consistent with the correct expression, which is $1/k$ times $f_1(\theta, \phi; {}^3P_g)$, appearing in their paper. At an energy 0.11 eV above threshold the present calculations *B* and *C* yield, respectively, cross sections of $2.43 \times 10^{-6} a_0^2$ and $3.28 \times 10^{-6} a_0^2$, which are much too low compared with the corresponding experimental value of $1.57 \times 10^{-4} a_0^2$ of Burrow,³ whereas the BO calculation of Becker and Dahler gives a cross section which is smaller than the measured value by only a factor of about 7 and which appears to be better than ours. At this point we wish to remark that the cross sections of Becker and Dahler are not reliable in the vicinity of threshold, because they have adopted energy eigenvalues which are not close enough to the corresponding experimental data. On the other hand, in spite of our adoption of experimental energies, we find that near threshold the present cross sections are too low compared to the experimental results,³ which are reported to be uncertain by a factor of 2. In Table II the BO slopes near threshold are given. It is seen that the present BO slopes are also very small in comparison with experiment. Therefore we conclude that the BO method is incapable of predicting reliable cross sections near threshold. Furthermore, Becker and Dahler observed that the calculated cross sections are independent of which of the two different sets of hydrogenic wave functions they used. But it is seen from Fig. 1 that the cross sections are sensitive to the wave func-

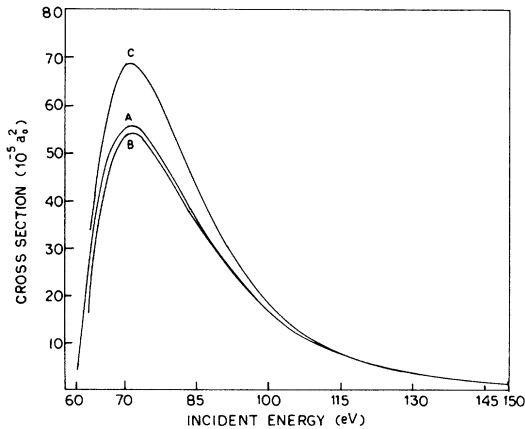


FIG. 1. Total cross sections for the electron-impact ${}^3P(2p)^2 \rightarrow {}^1S(1s)^2$ transition in helium. Curve *A* refers to the BO calculation of Becker and Dahler (Ref. 2). Curves *B* and *C* display the results of present BO calculations using form *A* and form *B*, respectively, for the atomic wave functions (experimental eigenenergies are used).

tions we used (curves *B* and *C*) in the immediate vicinity of threshold.

B. Close-coupling calculation

The close-coupled equations (19) and (20) are reduced to a set of linear simultaneous algebraic equations using the method adopted in Refs. 5 and 6. The resulting equations are then solved by the matrix inversion method. In this calculation we have adopted for the atomic wave functions form *B* and used experimental energies for the target eigenstates. The partial-wave matrix elements $B^L(k'\tau'; k\tau)$ occurring in the close-coupling equations are calculated using the method published by Lyons and Nesbet.^{18,19} The details are described in the Appendix.

Figure 2 shows a comparison of the results of present close-coupling calculation (curve 1) with those of Becker and Dahler² (curve 2) calculated using a one-parameter ground-state wave function for helium. Near threshold our cross sections rise steeply, in sharp contrast to the findings of Becker and Dahler. At an energy nearly 15 eV beyond threshold, the two calculations give cross

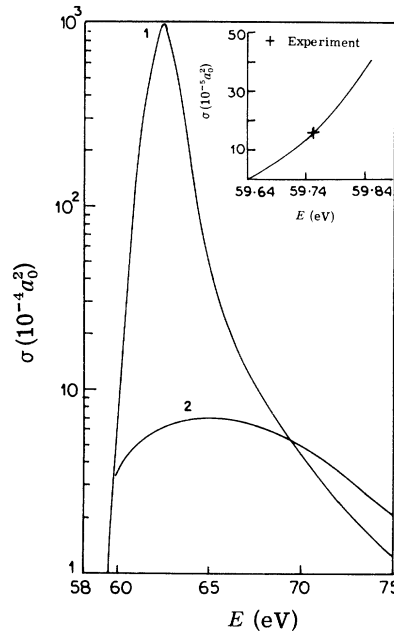


FIG. 2. Total cross section vs incident electron energy for the electron-impact ${}^3P(2p)^2 \rightarrow {}^1S(1s)^2$ transition in helium. Curve 1 represents the present close-coupling (CC) cross sections; curve 2 displays the CC results of Becker and Dahler (Ref. 2). Inset: Comparison of present CC results with experiment (Ref. 3) in the immediate neighborhood of threshold. The experimental result (Ref. 3) is reported to be uncertain by a factor of 2.

TABLE II. Comparison of experimental slopes $\Delta\sigma/\Delta E$ in units of cm^2/eV with the theoretical slopes calculated using BO and CC cross sections.

Energy above threshold (eV)	BO ^a	Present work BO ^b	CC	Experiment ^c
0.11	1.8×10^{-21}	1.2×10^{-21}	6×10^{-20}	4×10^{-20}

^a Calculation A (see Sec. III A); slope obtained from BO cross sections of Ref. 2.

^b Calculation C (see Sec. III A); slope obtained from present BO cross sections calculated using form- B wave functions.

^c Reference 3.

sections which tend to agree closely. The discrepancy can be explained easily; near threshold the results of Ref. 2 are not reliable because of the adoption of a threshold energy which is not very close to experiment. Far from threshold, where the effect of slight shift of threshold is not appreciable, the two calculations should agree closely.

A comparison of our results (see Table I) with experiment shows that the present close-coupling cross section is in good agreement with the measured value. As expected, near threshold our calculated slope (see Table II) is also in good agreement with the experimental slope.

In the present case of parity-unfavored transition both the BO and CC differential cross sections are proportional to the square of the sine of the scattering angle. When plotted against θ these cross sections will therefore show a nature similar to the $\sin^2\theta$ curve.

C. Threshold behavior of cross sections

Kulander and Dahler¹² have studied threshold behavior of cross sections for parity-unfavored transitions. In the present case of double excitation, cross sections are expected to vary as k^3 for quite some distance beyond threshold. A close look at our cross sections (Table I) reveals that the present calculations yield results which are consistent with the threshold law for parity-unfavored transitions.

IV. CONCLUSION

In the present investigation we find that the BO method fails to predict reliable cross sections near threshold. The present calculation indicates that at a distance nearly 15 eV beyond threshold the predictions of BO theory are in substantial agreement with the results of the presumably more accurate close-coupling method. The reason for this apparent success of the BO method at a little distance beyond threshold is given by Kulander and Dahler.¹² We further observe that close to threshold BO cross sections are sensitive to the wave functions we used. This is consistent with the conclusion of Shelton *et al.*²⁰ that in the case of

spin-forbidden transition, e.g., excitation of the ${}^3P(1s2p)$ state of helium, cross sections are quite sensitive to the choice of atomic wave functions.

One of the striking features of the present close-coupling calculations is that near threshold cross sections rise steeply, in sharp contrast to the results of Becker and Dahler. We remark that the calculations of Becker and Dahler will not be applicable in the immediate neighborhood of threshold because of the adoption of a threshold energy which is not sufficiently close to the experimental value. Near threshold our close-coupling cross sections are sometimes about 50 or 60 times as large as those of Becker and Dahler, and this large difference cannot be attributed to the choice of wave functions. We further observe that even a two-state calculation such as ours yields results in good agreement with experiment. Since the experimental cross sections are reported to be uncertain by a factor of 2, it will be difficult to comment upon the effect of coupling of other states in the present situation. Moreover, the experimental results available are very scanty; this is why it has not been possible to say anything definite about the success of a particular method. Precise experimental measurement is desirable for testing the validity of the present two-state close-coupling method in the neighborhood of threshold.

ACKNOWLEDGMENT

The authors wish to thank Dr. A. S. Ghosh for valuable discussions of computer programming.

APPENDIX A: EVALUATION OF PARTIAL-WAVE MATRIX ELEMENTS

Becker and Dahler² have remarked that when the atomic wave function is approximated by a product of orbitals appropriate to a single atomic configuration, e.g., to the configuration ${}^3P(2p)^2$, only one partial wave ($l=l'=L=1$) contributes to the cross section. Here we arrive at the same conclusion while explicitly evaluating the matrix element.

With T replaced by B in (14) in Sec. II we have the partial-wave expansion

$$\langle \hat{k}' n' l'_a m'_a | B | \hat{k} n l_a m_a \rangle = N' (kk')^{-1/2} \sum_{LM} \sum_{l'm'} \sum_{im} \langle l' l'_a m' m'_a | LM \rangle Y_{l'm'}(\hat{k}') B^L(k'n'l'_a; knl_a) \langle l_a m m_a | LM \rangle Y_{lm}^*(\hat{k}). \quad (\text{A1})$$

Using the orthogonality properties of the spherical harmonics and Clebsch-Gordan coefficients, we invert Eq. (A1) and get

$$B^L(k'n'l'_a; knl_a) = \frac{(kk')^{1/2}}{N'} \int d\hat{k}' d\hat{k} \sum_{m'm'_a} \sum_{mm_a} \langle l' l'_a m' m'_a | LM \rangle \langle l_a m m_a | LM \rangle Y_{l'm'}^*(\hat{k}') Y_{lm}(\hat{k}) \langle \hat{k}' n' l'_a m'_a | B | \hat{k} n l_a m_a \rangle. \quad (\text{A2})$$

Let us now calculate the partial-wave matrix element for the ${}^3P(2p)^2 \leftarrow {}^1S(1s)^2$ transition. We have

$$B^L(k', 2, l', 1; k, 1, l, 0) = \frac{(kk')^{1/2}}{N'} \int d\hat{k}' d\hat{k} \sum_{m'm'_a} \sum_{mm_a} \langle l', 1, m', m'_a | L, M \rangle \langle l, 0, m, 0 | L, M \rangle \times Y_{l'm'}^*(\hat{k}') Y_{lm}(\hat{k}) \langle \hat{k}', 2, 1, m'_a | B | \hat{k}, 1, 0, 0 \rangle. \quad (\text{A3})$$

Considering a typical term of the ground-state wave function for helium, using (11), (12), and (9) of Sec. II, expanding $e^{i\hat{k} \cdot \hat{r}}$ and electron-electron interaction terms of Eq. (9) in terms of spherical harmonics, we find that of all of the terms in the operator $H - E$ only $1/r_{23}$ provides a nonvanishing contribution to B^L . Equation (A3) then takes the form

$$\begin{aligned} B^L(k', 2, l', 1; k, 1, l, 0) &= \int d\hat{k}' d\hat{k} \sum_{mm'_a} \langle l, 1, m', m'_a | L, M \rangle \delta_{l, L} Y_{l'm'}^*(\hat{k}') Y_{lm}(\hat{k}) \\ &\times \int d\hat{r}_1 d\hat{r}_2 d\hat{r}_3 \sum_{\nu'} \langle 1, 1, \nu', m'_a - \nu' | 1, m'_a \rangle r_1^\nu r_2^{\nu'} r_3^{\nu''} e^{-\alpha r_1 - \beta r_2 - \delta r_3} Y_{1, \nu'}^*(\hat{r}_1) Y_{1, m'_a - \nu'}^*(\hat{r}_2) \\ &\times \sum_{l\mu} i^l j_l(kr_1) Y_{l, \mu}(\hat{k}) Y_{l, \mu}(\hat{r}_1) \sum_{l'\mu'} (-i)^{l'} j_{l'}(k'r_3) Y_{l', \mu'}^*(\hat{k}') Y_{l', \mu'}(\hat{r}_3) \\ &\times \sum_{l_1 \mu_1} g_{l_1}(r_2, r_3) \frac{1}{2l_1 + 1} Y_{l_1, \mu_1}^*(r_2) Y_{l_1, \mu_1}(r_3), \end{aligned} \quad (\text{A4})$$

where we have used the expansion

$$\frac{1}{r_{ij}} = \sum_{l_1 \mu_1} g_{l_1}(r_i, r_j) \frac{4\pi}{2l_1 + 1} Y_{l_1, \mu_1}^*(\hat{r}_i) Y_{l_1, \mu_1}(\hat{r}_j),$$

$$g_{l_1}(r_i, r_j) = (1/r_>)(r_</r_>)^{l_1},$$

with $r_>$ and $r_<$ the greater or lesser, respectively, of r_i and r_j . Using the orthogonality of spherical harmonics we carry through the angular integrations over \hat{r}_1 , \hat{r}_2 , \hat{r}_3 , \hat{k} , and \hat{k}' . We see that $B^L(k', 2, l', 1; k, 1, l, 0)$ vanishes unless $l = l' = L = 1$.

A close inspection at the close-coupled equations (19) and (20) shows that $T^L(k', 2, l', 1; k, 1, l, 0)$ survives only when $l = l' = L = 1$. The radial integral R which is yet to be performed is the following:

$$R = \int dr_1 dr_2 dr_3 r_1^\beta r_2^{\alpha'} r_3^{\delta'} e^{-\alpha r_1 - \beta r_2 - \delta r_3} \times j_1(kr_1) j_1(k'r_3) g_1(r_2, r_3). \quad (\text{A5})$$

Now the integral R can be expressed in terms of G and W integrals,¹⁸

$$R = G(1, p' + 1 | k, \alpha) \left(\frac{\Gamma(q' + 2)}{\beta^{q' + 2}} G(1, s' - 1 | k', \delta) - W(1; q' + 1, s' - 1 | k', \beta, \delta) + W(1; q' - 2, s' + 1 | k', \beta, \delta) \right), \quad (\text{A6})$$

with

$$G(\lambda, p | k, \alpha) = \int_0^\infty dr j_\lambda(kr) r^{p-\lambda} e^{-\alpha r},$$

$$W(\lambda; p, g | k, \alpha, \beta) = \int_0^\infty dr j_\lambda(kr) A_p(\alpha, r) r^{\alpha-\lambda} e^{-\beta r},$$

where

$$A_p(\alpha, r) = \int_r^\infty s^p e^{-\alpha s} ds.$$

Similarly, all other partial-wave matrix elements can be expressed in terms of six basic integrals¹⁸ $G, H, I, V, W,$ and X , which are computed numerically according to the method prescribed by Lyons and Nesbet.^{18,19} In the present case ($\lambda=1$) we have, however, evaluated the G integrals analytically and used the analytical form of G to compute other integrals.

*On leave of absence from Department of Physics, University of Kalyani, Kalyani, West Bengal, India.

¹P. M. Becker and J. S. Dahler, Phys. Rev. Lett. 10, 491 (1963).

²P. M. Becker and J. S. Dahler, Phys. Rev. 136, A73 (1964).

³P. D. Burrow, Phys. Rev. A 2, 1774 (1970).

⁴I. H. Sloan and E. J. Moore, J. Phys. B 1, 414 (1968).

⁵A. S. Ghosh and D. Basu, Ind. J. Phys. 47, 765 (1973).

⁶J. Chaudhuri, A. S. Ghosh, and N. C. Sil, Phys. Rev. A 10, 2287 (1974).

⁷P. Mandal, A. S. Ghosh, and N. C. Sil, J. Phys. B 8, 2377 (1975).

⁸D. Basu, G. Banerji, and A. S. Ghosh, Phys. Rev. A 13, 1381 (1976).

⁹See, e.g., P. G. Burke and K. M. Smith, Rev. Mod. Phys. 34, 458 (1962).

¹⁰H. Massey and B. L. Moiseiwitsch, Proc. R. Soc. A 258, 147 (1960).

¹¹L. I. Schiff, *Quantum Mechanics* (McGraw-Hill, New York, 1955), Chap. 9, p. 244.

¹²K. C. Kulander and J. S. Dahler, Phys. Rev. A 6, 1436 (1972).

¹³G. F. Drukarev, *The Theory of Electron-Atom Collisions* (Academic, New York, 1965), Chap. 7, p. 118.

¹⁴Reference 11, p. 233.

¹⁵H. Massey and B. L. Moiseiwitsch, Proc. R. Soc. A 227, 38 (1954).

¹⁶Reference 13, p. 122.

¹⁷F. W. Byron, Jr., and C. J. Joachain, Phys. Rev. 146, 1 (1966).

¹⁸J. D. Lyons and R. K. Nesbet, J. Comput. Phys. 4, 499 (1969).

¹⁹J. D. Lyons and R. K. Nesbet, J. Comput. Phys. 11, 166 (1973).

²⁰W. N. Shelton, K. L. Baluja, and D. H. Madison, in *Abstracts of Papers of the Eighth International Conference on the Physics of Electronic and Atomic Collisions, Belgrade, 1973*, edited by B. C. Čobić and M. V. Kurepa, (Institute of Physics, Belgrade, 1973), p. 296.